Remote sensing of shallow-water bathymetry: Leveraging multispectral satellite ocean color observations

Jianwei Wei[1], Menghua Wang[2], Zhongping Lee[3], Henry O. Briceño[4], Xiaolong Yu[3], Lide Jiang[5], Junwei Wang[6], Kelly Luis[3], Rodrigo Garcia[3]

1.NOAA/STAR; GST Inc.; 2. NOAA/STAR; 3. University of Massachusetts Boston; 4. Florida International University; 5. NOAA/STAR; Colorado State University; 6. Xiamen University

Question and Objective

Ocean color satellites allow for derivation of important biogeochemical properties for global oceans. Limited to multispectral resolution, however, it remains difficult to generate geophysical properties, e.g., water depth, over global shallow waters with the satellite remote sensing reflectance ($R_{rs}(\lambda)$). This study evaluate a new algorithm for practical application of multispectral ocean color observations to the retrieval of water depth for optically shallow waters.

	Landsat-8	SNPP	Sentinel-3A
Ocean color sensor	OLI	VIIRS	OLCI
Visible bands	443, 482, 561, 655	410, 443, 486, 551, 638, 671	400, 413, 443, 490, 510, 560, 620, 665, 674, 681
Revisit	16 days	1 day	1-3 days
Data access	USGS	NOAA	NOAA
Processing software	SeaDAS/L2GEN	MSL12	MSL12
Atmospheric correction	NIR-SWIR	NIR-SWIR	NIR

Method and Algorithm

❑ Semi-analytical approach designed for hyperspectral $R_{rs}(\lambda)$

Ocean color community has invested great effort in shallow water remote sensing with semi-analytical algorithms. An extensively tested algorithm is the so-called hyperspectral optimization processing exemplar (HOPE) (Lee et al., 1998; 1999). A shallow-water reflectance model is established as:

$$r_{rs}(\lambda) \approx r_{rs}^{dp}(\lambda)\cdot\left\{1-\exp\left[-\left(\frac{1}{\cos\theta_w}+\frac{D_0\left(1+D_1\cdot u(\lambda)\right)^{0.5}}{\cos\theta_a}\right)\cdot k(\lambda)\cdot H\right]\right\}+$$
$$\frac{\rho(\lambda)}{\pi}\exp\left[-\left(\frac{1}{\cos\theta_w}+\frac{D_0'\left(1+D_1'\cdot u(\lambda)\right)^{0.5}}{\cos\theta_a}\right)\cdot k(\lambda)\cdot H\right]$$

Five unknowns of P, G, X, B, and H can be determined by quantifying the difference between the observed spectrum, $R_{rs}^{obs}(\lambda)$, and modeled spectrum, $R_{rs}^{mod}(\lambda)$,

$$err=\frac{\left[\sum\left(R_{rs}^{mod}(\lambda_i)-R_{rs}^{obs}(\lambda_i)\right)^2\right]^{1/2}}{\sum R_{rs}^{obs}(\lambda_i)}$$

Cost function

❑ Two-spectrum optimization approach (2-SOA) for multispectral $R_{rs}(\lambda)$

Our new algorithm incorporates two independent $R_{rs}(\lambda)$ spectra measured at the same location in the spectral optimization, thus allowing to generate much improved estimation for water depth with multispectral satellite ocean color observations. The work-flow is schematically shown in below:

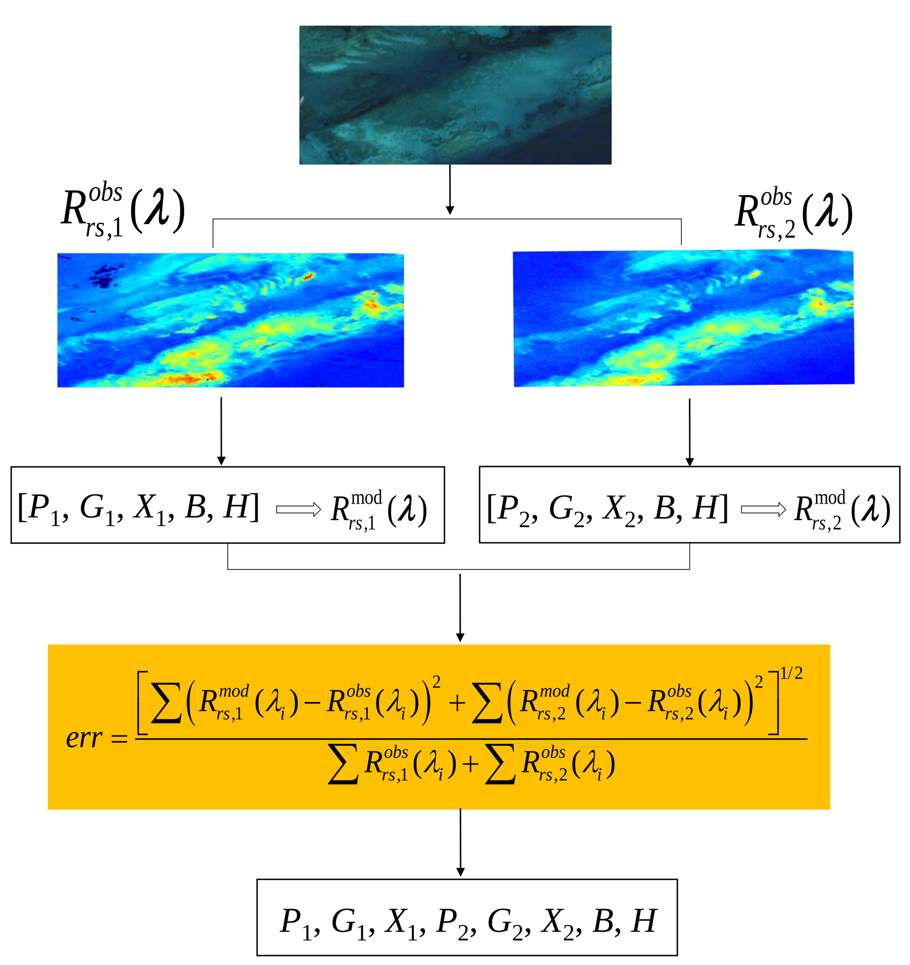

P: phytoplankton light absorption; G: CDOM light absorption; X: particle backscattering; B: bottom albedo; H: depth

Performance Evaluation

Hyperspectral $R_{rs}(\lambda)$ data are synthesized to cover a wide range of depths, three benthic types (coral, seagrass, and sand), and turbidity. These $R_{rs}(\lambda)$ data are then interpolated to represent the measurements for Landsat-8/OLI, SNPP/VIIRS, and Sentinel-3A/OLCI.

Parameters	Range (interval)	Levels
P	0.01–0.19 (0.03)	7
G	0.01–0.19 (0.03)	7
X	0.001–0.019 (0.004)	7
H	0.5–29.5 (1.0)	30
η	−0.5–2.5 (0.5)	7
S_{dg}	0.015	1
θ_a	30°	1
B: coral	0.005, 0.05, 0.1	3
B: seagrass	0.01, 0.035, 0.08	3
B: sand	0.1, 0.25, 0.6	3

	Lower boundary	Upper boundary	Initial value
P_1	0.005	0.35	$0.072\cdot[R_{rs,1}(443)/R_{rs,1}(550)]^{-1.62}$
G_1	0.001	0.6	$0.072\cdot[R_{rs,1}(443)/R_{rs,1}(550)]^{-1.62}$
X_1	0.0001	0.08	$30\cdot a_w(670)\cdot R_{rs,1}(670)$
P_2	0.005	0.35	$0.072\cdot[R_{rs,2}(443)/R_{rs,2}(550)]^{-1.62}$
G_2	0.001	0.6	$0.072\cdot[R_{rs,2}(443)/R_{rs,2}(550)]^{-1.62}$
X_2	0.0001	0.08	$30\cdot a_w(670)\cdot R_{rs,2}(670)$
B	0.001	0.8	0.5
H	0.1	30.5	10

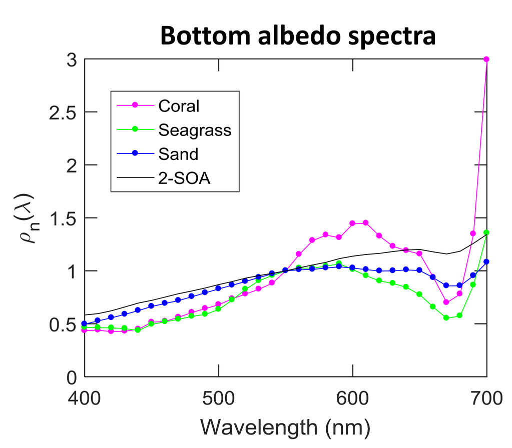

- ❖ The bottom albedo spectra for coral, seagrass, and sand were derived from Hochberg et al. (2003).
- ❖ 2-SOA uses a fixed bottom albedo spectrum (bright band) (Lee et al., 1999).
- ❖ 2-SOA used fixed lower and upper constraints and dynamic initial values.

❑ Error statistics for model-estimated water depth (0.5-30 m)

		Landsat-8\OLI			SNPP\VIIRS			Sentinel-3A\OLCI		
		coral	seagrass	sand	coral	seagrass	sand	coral	seagrass	sand
Standard	MAPE	42%	43%	21%	22%	31%	13%	22%	26%	10%
	Bias	14%	13%	7%	6%	18%	2%	5%	14%	3%
	RMSE	9.3	9.5	6.0	8.8	9.1	4.6	8.3	8.5	4.1
This study	MAPE	26%	28%	15%	14%	19%	11%	14%	16%	10%
	Bias	1%	1%	3%	4%	9%	0%	1%	5%	2%
	RMSE	8.3	8.7	5.2	7.7	8.2	4.0	7.2	7.8	3.9

MAPE: median absolute percentage error; RMSE: root mean square error.

❑ Depth-specific error statistics for model-estimated water depth

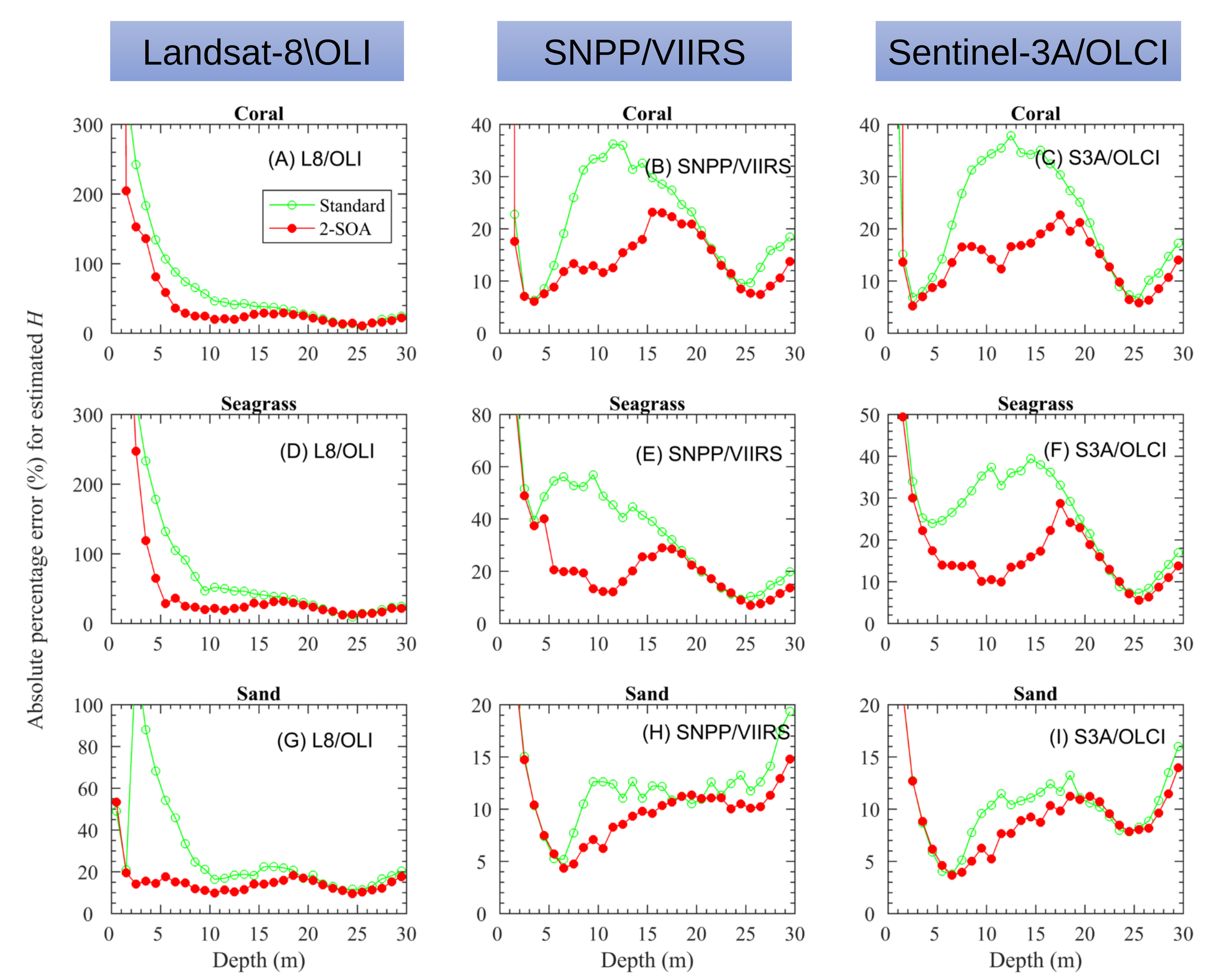

The algorithm performance varies with the range of water depth under study. Improved performance is observed for water depths over ~3-20 m in comparison to the "standard" approach.

Bathymetry from Satellite Images

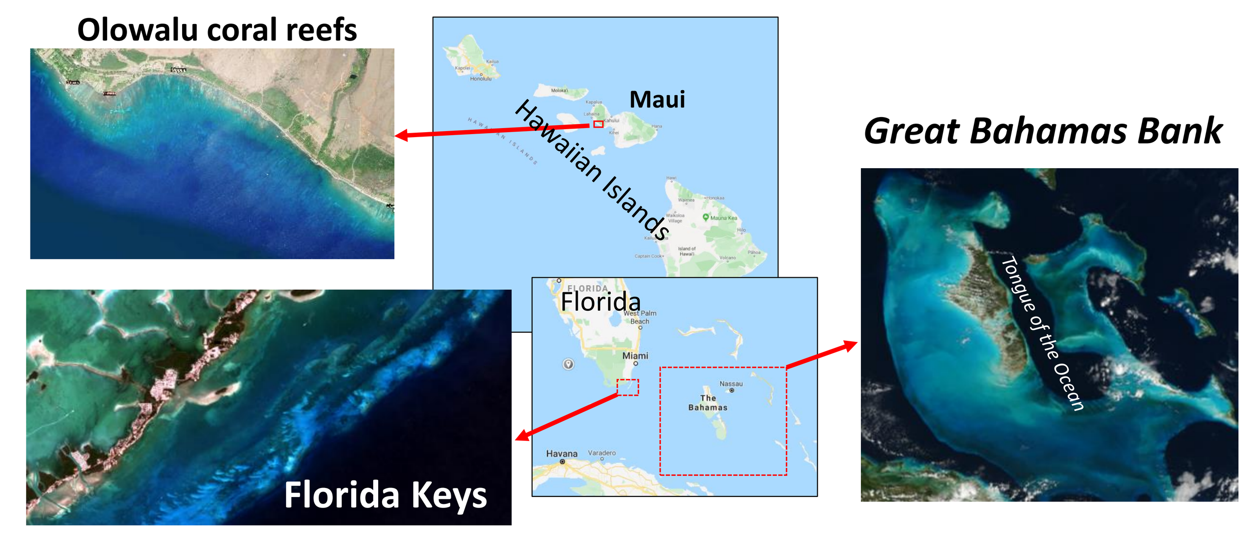

❑ Olowalu Reef (Maui, Hawaii)

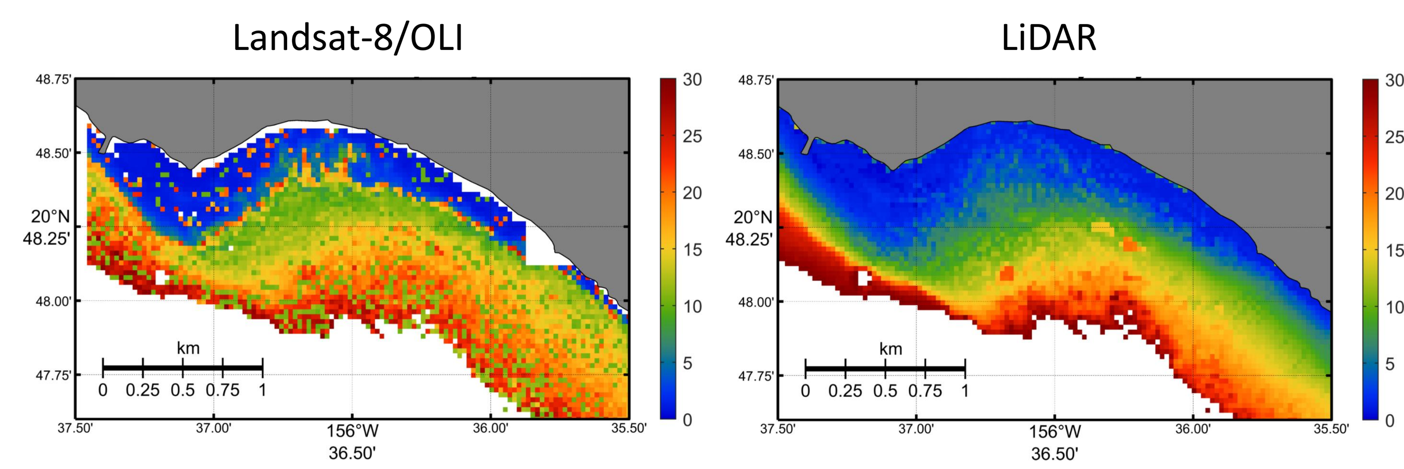

Error statistics for Landsat-8\OLI bathymetry and LiDAR data: MAPE = 40%, Bias = −17%, and RMSE = 8.4 m.

❑ Florida Keys

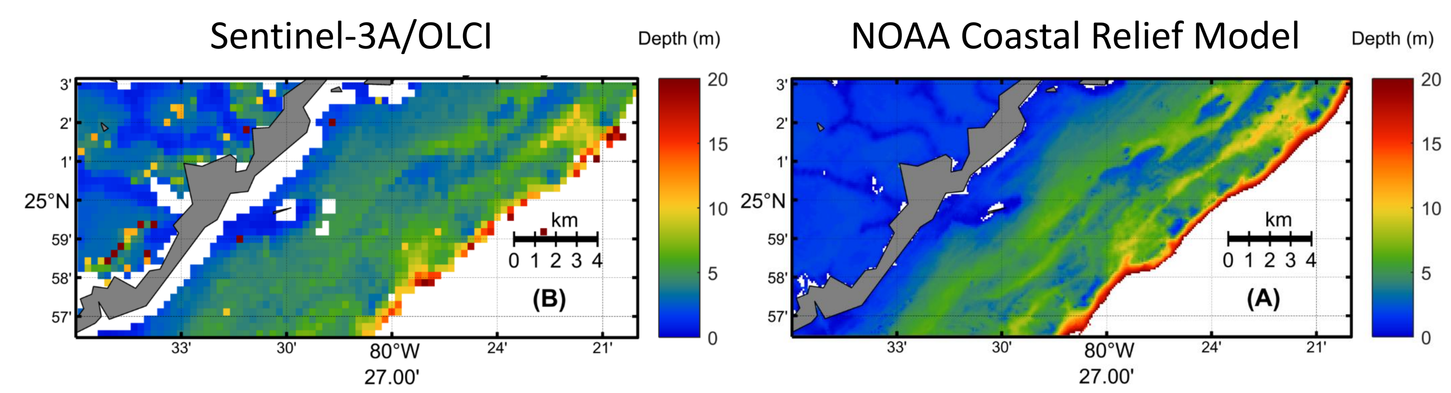

Error statistics for Sentinel-3A/OLCI bathymetry and NOAA CRM model: MAPE = 16%, Bias = −2.7%, and RMSE = 2 m.

❑ The Bahamas

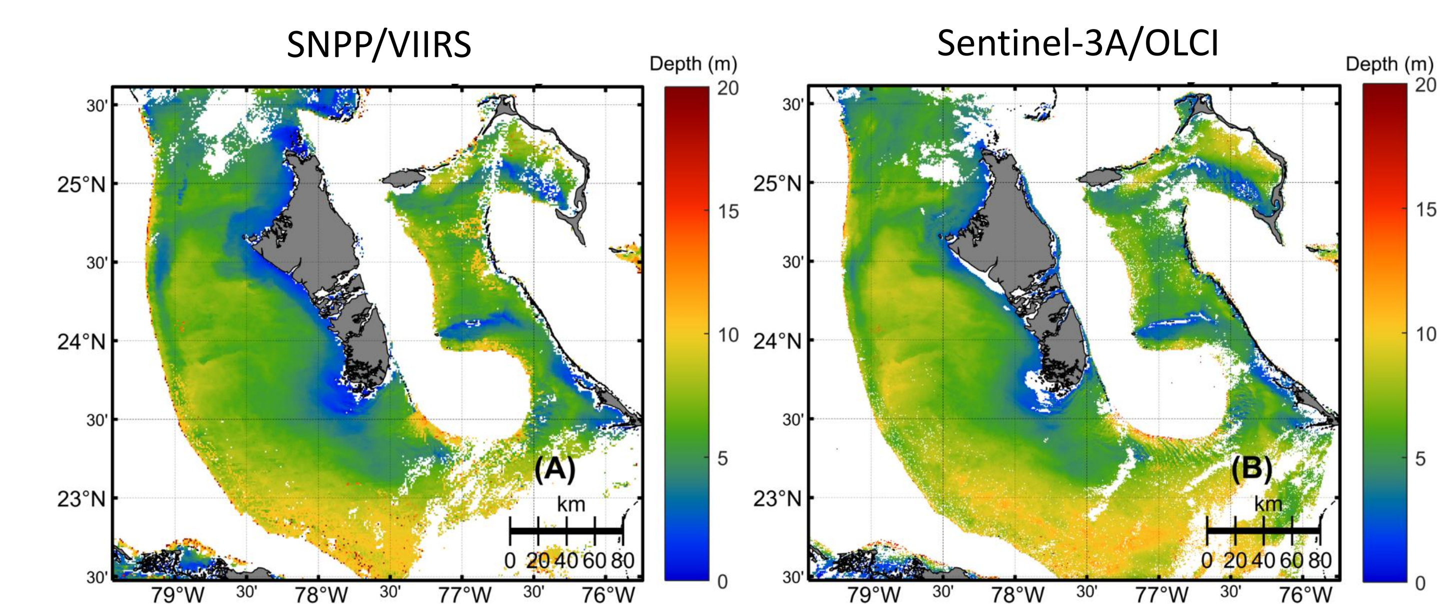

Error statistics for SNPP/VIIRS bathymetry and Sentinel-3A/OLCI bathymetry: MAPE = 9%, Bias = 8%, and RMSE = 0.57 m.

Conclusions

- ❑ A new algorithm is developed for shallow-water bathymetric estimation for multispectral satellite ocean color sensors.
- ❑ Evaluation shows substantial improvement in the estimated depth product over 0-30 m.

Acknowledgment: http://www.soest.hawaii.edu/coasts